Resonant Phonon Excitation in Bilayer Graphene

Contact *Isabella.Gierz@mpsd.mpg.de*

Isabella Gierz
Max Planck Institute for the Structure and Dynamics of Matter
Luruper Chaussee 149, 22761 Hamburg, Germany

Matteo Mitrano
Max Planck Institute for the Structure and Dynamics of Matter
Luruper Chaussee 149, 22761 Hamburg, Germany

Hubertus Bromberger
Max Planck Institute for the Structure and Dynamics of Matter
Luruper Chaussee 149, 22761 Hamburg, Germany

Cephise Cacho
Central Laser Facility, STFC Rutherford Appleton Laboratory
Harwell Oxford, Didcot, OX11 0QX, United Kingdom

Richard Chapman
Central Laser Facility, STFC Rutherford Appleton Laboratory
Harwell Oxford, Didcot, OX11 0QX, United Kingdom

Emma Springate
Central Laser Facility, STFC Rutherford Appleton Laboratory
Harwell Oxford, Didcot, OX11 0QX, United Kingdom

Stefan Link
Max Planck Institute for Solid State Research
Heisenbergstr. 1, 70569 Stuttgart, Germany

Ulrich Starke
Max Planck Institute for Solid State Research
Heisenbergstr. 1, 70569 Stuttgart, Germany

Andrea Cavalleri
Max Planck Institute for the Structure and Dynamics of Matter
Luruper Chaussee 149, 22761 Hamburg, Germany

Department of Physics, Clarendon Laboratory, University of Oxford
Parks Rd. Oxford, OX1 3PU, United Kingdom

Introduction

Phonon pumping has evolved into a powerful tool to control the electronic properties of solids. For example, phonon pumping has been used to induce transient superconducting states in $La_{1.8-x}Eu_{0.2}Sr_xCuO_4$ [1] and $YBCO_{6+\delta}$ [2] or insulator-metal transitions in $NdNiO_3/LaAlO_3$ [3] and $Pr_{1-x}Ca_xMnO$ [4].

Bilayer graphene posseses two IR-active modes (the in-plane E_{1u} mode at 6.3µm and the out-of-plane A_{2u} mode at 11.5µm) that can be exploited for electronic structure control. The in-plane mode has attracted a lot of attention because of its Fanø lineshape that indicates the presence of a symmetry-forbidden coupling to electronic interband transitions, and its surprisingly strong oscillator strength that has been attributed to the charged phonon effect [5]. Furthermore, in the presence of a broken inversion symmetry induced by charge doping, the E_{1u} mode mixes with the Raman-active E_{2g} mode [6] that is responsible for the kink in graphene's linear electronic dispersion [7]. The frequency of the in-plane mode can be easily reached with an optical parametric amplifier (OPA) combined with difference frequency generation (DFG), and the mode can be pumped efficiently by a laser beam at normal incidence, assuring high pump fluences.

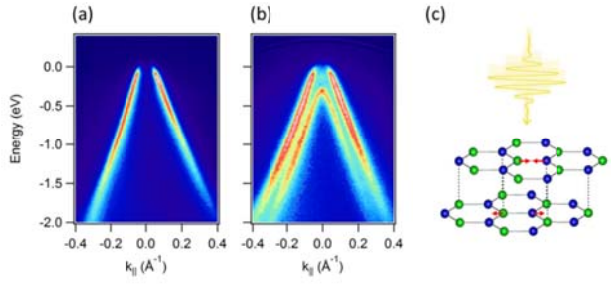

Fig. 1: Equilibrium band structure measured with HeIIα radiation of a hydrogen-intercalated graphene monolayer (a) and bilayer (b). Sketch of the resonantly excited in-plane E_{1u} lattice vibration (c).

Samples and Methods

For the present investigation we used quasi-freestanding epitaxial graphene monolayers and bilayers grown on the silicon-terminated face of silicon carbide (SiC) [8]. Prior to graphene growth, the SiC substrate was hydrogen-etched to remove scratches from mechanical polishing, resulting in atomically flat terraces. In a second step, the substrate was graphitized in argon atmosphere, and the resulting carbon layer(s) was (were) decoupled from the substrate by hydrogen intercalation. After growth, the samples were characterized with angle-resolved photoemission spectroscopy. The measured band structures for the obtained monolayer and bilayer samples are shown in Fig. 1a and b, respectively. The measurements were done along a cut through the K-point at the corner of the hexagonal Brillouin zone perpendicular to the ΓK-direction using HeIIα radiation at $\hbar\omega$=40.8eV at room temperature. Both samples are lightly hole-doped due to charge transfer from the substrate with the top of the valence band ~200meV above the Fermi level.

Figure 1c sketches the lattice displacement driven by a laser pulse resonant to the E_{1u} phonon. The two triangluar sublattices shown in green and blue move in opposite directions along the direction of the light field, resulting in a periodic modulation of the nearest neighbour distance. The sublattices in the top and bottom layer move out-of-phase, making the mode IR-active [9].

We have excited the graphene samples at various wavelengths in the mid-infrared (MIR) between λ_{pump}=4µm and λ_{pump}=9µm and probed the resulting redistribution of charge carriers with time- and angle-resolved photoemission spectroscopy (tr-ARPES). The setup consists of a Ti:Sa laser system (780nm, 1kHz, 30fs, 15mJ) where part of the light is converted to MIR frequencies using an OPA with DFG stage for the pump. The other part is focused on an argon gas jet for high-order harmonics generation and passed through a time-preserving grating monochromator to select a single harmonic at $\hbar\omega_{probe}$=31eV for the probe [10]. The probe ejects photoelectrons from the sample whose energies and momenta are determined by a hemispherical analyzer, giving direct access to the occupied part of the electronic band structure. All time-resolved experiments have been performed at 30K.

Results

In Fig. 2 we present snapshots of the band structure (upper panel) of bilayer graphene together with the pump-induced changes of the photocurrent (lower panel) for different pump-probe delays after excitation at λ_{pump}=6.3µm, resonant to the E_{1u} lattice vibration. The snapshots are taken along the ΓK-direction, where only two of the four π-bands are visible due to photemission matrix element effects [11]. In the present work

t=0fs corresponds to the peak of the pump-probe signal. With the equilibrium Fermi level located in the valence band, the pump pulse - aside from modulating the atomic positions - heats the electron gas via free carrier absorption [12]. Hence, the pump-probe signal is dominated by the associated broadening of the Fermi-Dirac distribution accompanied by a broadening of the band structure.

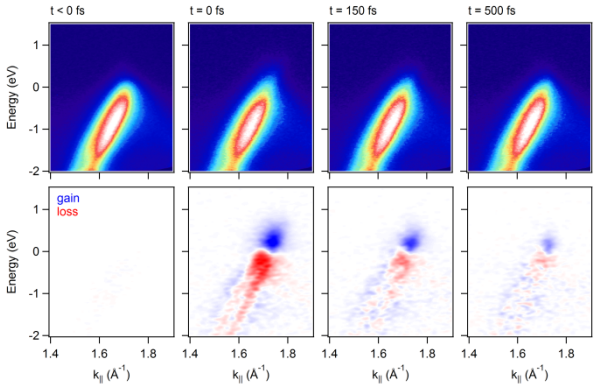

Fig. 2: Snapshots of the electronic structure of bilayer graphene for different pump-probe delays (upper panel) together with the corresponding pump-probe signal (lower panel). The excitation wavelength is 6.3µm in resonance with the in-plane E_{1u} lattice vibration.

For further analysis the snapshots in Fig. 2 are integrated over momentum and plotted as a function of pump-probe delay in Fig. 3a. At each time delay the momentum-integrated photocurrent is fitted by a Fermi-Dirac distribution to obtain the electronic temperature as a function of time (see Fig. 3b). Ref. [13] pointed out that this procedure is only strictly valid for a single band with a constant density of states at the Fermi level. If there are several bands close to E_F, like in the present case, the authors proposed to determine the spectral weight of each band separately before fitting with a Fermi-Dirac distribution. Unfortunately, the two bands are not clearly resolved in our data, so that this procedure is not easily applicable. To avoid confusion with a precise determination of the electronic temperature the fit results are labelled 'Fermi Width' in Fig. 3b. We have fitted the time evolution of the Fermi width with a double exponential decay that describes the cooling of the hot electronic distribution via the emission of optical (fast time constant τ_1 [14]) and acoustic phonons (slow time constant τ_2 [15]).

In order to find out whether excitation at resonance to the E_{1u} mode has any effect other than heating of the electronic distribution via free carrier absorption, we performed a wavelength-dependent study at constant pump fluence (F=0.26mJ/cm^2). The data were anaylized in the same way as described in the context of Figs. 3a and b. The wavelength dependence of the peak electronic temperature, max T_e, and of the fast relaxation time, τ_1, are plotted in Figs. 3c and d, respectively. Both quantities exhibit a minimum at resonance to the E_{1u} mode at λ_{pump}=6.3µm. The slow relaxation time, τ_2, is found to be independent of pump wavelength within the experimental error bars and is not shown here.

Discussion

In the free carrier absorption regime the peak electronic temperature is determined by the pump fluence [12]. The variation of max T_e with pump wavelength at constant pump fluence therefore indicates that, at resonance with the E_{1u} phonon, the observed pump-probe signal has an additional contribution from coherent lattice vibrations. The decrease in max T_e at resonance might originate from a transient change of the electronic dispersion as suggested by frozen phonon calculations (not shown here). However, the phonon period of 21fs is shorter than the probe pulse duration of 30fs, so that the band structure changes could not be resolved in the present experiment.

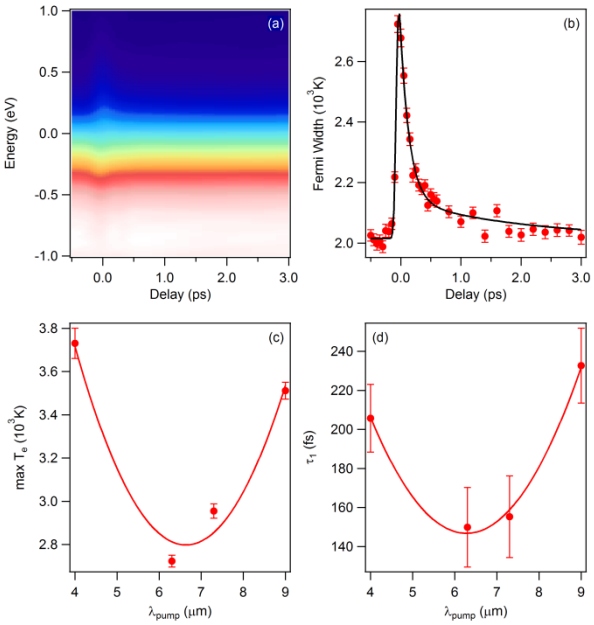

Fig. 3: (a) Momentum-integrated photocurrent in bilayer graphene at λ_{pump}=6.3µm as a function of energy and pump-probe delay in the vicinity of the Fermi level. (b) Width of the Fermi-Dirac distribution as a function of pump-probe delay. (c) Dependence of the maximum electronic temperature on excitation wavelength for constant excitation fluence of 0.26mJ/cm^2. (d) Dependence of the fast relaxation time τ_1 on excitation wavelength for constant excitation fluence of 0.26mJ/cm^2 of the Fermi level.

The minimum in the fast relaxation time τ_1 indicates an enhanced scattering rate between electrons and optical phonons at resonance with the E_{1u} lattice vibration. According to Ref. [16] the scattering rate due to electron-phonon coupling is given by

$$\boldsymbol{1/\tau = 2\pi \int_0^\infty \alpha^2(\omega')F(\omega')[2N(\omega') + f(\omega' - \omega) + f(\omega' + \omega)]d\omega',}$$

where $\boldsymbol{\alpha^2(\omega)F(\omega)}$ is the Eliashberg function, $\boldsymbol{N(\omega)}$ is the Bose-Einstein distribution, and $\boldsymbol{f(\omega)}$ is the Fermi-Dirac distribution. Both $\boldsymbol{N(\omega)}$ and $\boldsymbol{f(\omega)}$ depend on temperature.

A comparison with monolayer graphene (data not shown), where the in-plane lattice vibration cannot be resonantly driven with light and where neither τ_1 nor max T_e depend on pump wavelength, indicates that an elevated electronic temperature alone cannot explain our findings.

Our pump pulse resonantly excites E_{1u} lattice vibrations and, hence, changes the phonon distribution function $\boldsymbol{N(\omega)}$. In addition we expect significant changes of the electronic structure due to E_{1u} lattice displacement that will affect the Elishberg function $\boldsymbol{\alpha^2(\omega)F(\omega)}$. We believe that the interplay of both contributions is responsible for the observed wavelength dependence of max T_e.

Summary

In summary, we have excited monolayer and bilayer graphene at MIR wavelengths between 4µm and 9µm, both on- and off-resonance with the in-plane E_{1u} mode in bilayer graphene, and probed the response of the electronic structure with tr-ARPES. We find that both the peak electronic temperature max T_e as well as the fast relaxation time τ_1 commonly attributed to the coupling to optical phonons exhibit a minimum at resonance with the E_{1u} mode. The absence of any pump wavelength dependence in monolayer graphene, where the in-plane lattice vibration cannot be resonantly excited with light, indicates that the effect has to be attributed to coherent phonon oscillations.

Conclusion

The present experiment shows that control of the electronic properties via phonon-pumping is not restricted to strongly

correlated materials. On the contrary, any atomic displacement should directly result in changes of the electronic structure of the respective solid. Aside from strongly correlated materials, such changes are particularly large in graphene and in the family of transition metal dichalcogenides, opening up new avenues for electronic structure control with light.

Acknowledgements

The research leading to these results has received funding from LASERLAB-EUROPE (grant agreement no. 284464, EC's Seventh Framework Programme).

References

1. D. Fausti, R. I. Tobey, N. Dean, S. Kaiser, A. Dienst, M. C. Hoffmann, S. Pyon, T. Takayama, H. Takagi, and A. Cavalleri, Science 331,189 (2011)
2. W. Hu, S. Kaiser, D. Nicoletti, C. R. Hunt, I. Gierz, M. C. Hoffmann, M. Le Tacon, T. Loew, B. Keimer, and A. Cavalleri, *Nat. Mater.* **13**, 705 (2014); S. Kaiser, C. R. Hunt, D. Nicoletti, W. Hu, I. Gierz, H. Y. Liu, M. Le Tacon, T. Loew, D. Haug, B. Keimer, and A. Cavalleri, *Phys. Rev. B* **89**, 184516 (2014)
3. A. D. Caviglia, R. Scherwitzl, P. Popovich,W. Hu, H. Bromberger, R. Singla, M. Mitrano, M. C. Hoffmann, S. Kaiser, P. Zubko, S. Gariglio, J.-M. Triscone, M. Först, and A. Cavalleri, *Phys. Rev. Lett.* **108**, 136801 (2012)
4. M. Rini, R. Tobey, N. Dean, J. Itatani, Y. Tomioka, Y. Tokura, R. W. Schoenlein, and A. Cavalleri, *Nature* **449**, 72 (2007)
5. Y. Zhang, T.-T. Tang, C. Girit, Z. Hao, M. C. Martin, A. Zett, M. F. Crommie, Y. R. Shen, and F. Wang, *Nature* **459**, 820 (2009); A. B. Kuzmenko, L. Benfatto, E. Cappelluti, I. Crassee, D. van der Marel, P. Blake, K. S. Novoselov, and A. K. Geim, *Phys. Rev. Lett.* **103**, 116804 (2009); T.-T. Tang, Y. Zhang, C.-H. Park, B. Geng, C. Girit, Z. Hao, M. C. Martin, A. Zettl, M. F. Crommie, S. G. Louie, Y. R. Shen, and F. Wang, *Nat. Nanotechnol.* **5**, 32 (2010)
6. L. M. Malard, D. C. Elias, E. S. Alves, and M. A. Pimenta, Phys. Rev. Lett. 101, 257401 (2008); T. Ando, and M. Koshino, J. Phys. Soc. Jpn. 78, 034709 (2009); P. Gava, M. Lazzeri, A. M. Saitta, and F. Mauri, *Phys. Rev. B* **80**, 155422 (2009); J. Yan, T. Villarson, E. A. Henriksen, P. Kim, and A. Pinczuk, *Phys. Rev. B* **80**, 241417(R) (2009)
7. A. Bostwick, T. Ohta, T. Seyller, K. Horn, and Eli Rotenberg, *Nat. Phys.* **3**, 36 (2007)
8. C. Riedl, C. Coletti, T. Iwasaki, A. A. Zakharov, and U. Starke, *Phys. Rev. Lett.* **103**, 246804 (2009)
9. A. C. Ferrari, and D. M. Basko, *Nat. Nanotechnol.* **8**, 235 (2013)
10. F. Frassetto, C. Cacho, C. A. Froud, I. C. E. Turcu, P. Villoresi, W. A. Bryan, E. Springate, and L. Poletto, *Opt. Express* **19**, 19169 (2011)
11. E. L. Shirley, L. J. Terminello, A. Santoni, and F. J. Himpsel, *Phys. Rev. B* **51**, 13614 (1995)
12. I. Gierz, J. C. Petersen, M. Mitrano, C. Cacho, I. C. E. Turcu, E. Springate, A. Stöhr, A. Köhler, U. Starke, and A. Cavalleri, *Nat. Mater.* **12**,1119 (2013)
13. S. Ulstrup, J. C. Johannsen, M. Grioni, and P. Hofmann, *Rev. Sci. Instrum.* **85**, 013907 (2014)
14. T. Kampfrath, L. Perfetti, F. Schapper, C. Frischkorn, and M. Wolf, *Phys. Rev. Lett.* **95**, 187403 (2005); H. Yan D. Song, K. F. Mak, I. Chatzakis, J. Maultzsch, and T. F. Heinz, Phys. Rev. B 80, 121403(R) (2009)
15. H. Yan D. Song, K. F. Mak, I. Chatzakis, J. Maultzsch, and T. F. Heinz, Phys. Rev. B 80, 121403(R) (2009); K. Kang, D. Abdula, D. G. Cahill, and M. Shim, *Phys. Rev. B* **81**, 165405 (2010); J. C. W. Song, M. Y. Reizer, and L. S. Levitov, *Phys. Rev. Lett.* **109**, 106602 (2012)
16. G. Grimvall, *Phys. Scr.* **14**, 63 (1976)